

Phase II Investigation of TVB-2640 (Denifanstat) with Bevacizumab in Patients with First Relapse High-Grade Astrocytoma



William Kelly¹, Adolfo Enrique Diaz Duque¹, Joel Michalek², Brandon Konkel³, Laura Cafilisch³, Yidong Chen², Sarath Chand Pathuri¹, Vinu Madhusudanannair-Kunnuparampil⁴, John Floyd II⁵, and Andrew Brenner¹

ABSTRACT

Purpose: Glioblastoma represents the most common primary brain tumor. Although antiangiogenics are used in the recurrent setting, they do not prolong survival. Glioblastoma is known to upregulate fatty acid synthase (FASN) to facilitate lipid biosynthesis. TVB-2640, a FASN inhibitor, impairs this activity.

Patients and Methods: We conducted a prospective, single-center, open-label, unblinded, phase II study of TVB-2640 plus bevacizumab in patients with recurrent high-grade astrocytoma. Patients were randomly assigned to TVB-2640 (100 mg/m² oral daily) plus bevacizumab (10 mg/kg i.v., D1 and D15) or bevacizumab monotherapy for cycle 1 only (28 days) for biomarker analysis. Thereafter, all patients received TVB-2640 plus bevacizumab until treatment-related toxicity or progressive disease (PD). The primary endpoint was progression-free survival (PFS).

Results: A total of 25 patients were enrolled. The most frequently reported adverse events (AE) were palmar-plantar erythrodysesthesia, hypertension, mucositis, dry eye, fatigue, and skin infection. Most were grade 1 or 2 in intensity. The overall response rate (ORR) for TVB-2640 plus bevacizumab was 56% (complete response, 17%; partial response, 39%). PFS6 for TVB-2640 plus bevacizumab was 31.4%. This represented a statistically significant improvement in PFS6 over historical bevacizumab monotherapy (BELOB 16%; $P = 0.008$) and met the primary study endpoint. The observed OS6 was 68%, with survival not reaching significance by log-rank test ($P = 0.56$).

Conclusions: In this phase II study of relapsed high-grade astrocytoma, TVB-2640 was found to be a well-tolerated oral drug that could be safely combined with bevacizumab. The favorable safety profile and response signals support the initiation of a larger multicenter trial of TVB-2640 plus bevacizumab in astrocytoma.

Introduction

Glioblastoma (grade 4 astrocytoma) is the most common and most aggressive primary brain malignancy in adults. The mainstay of treatment for newly diagnosed glioblastoma consists of maximal surgical resection of the primary tumor, followed by radiotherapy with concurrent temozolomide daily for 6 weeks followed by maintenance temozolomide for 6 months (1, 2). This combination of temozolomide plus radiotherapy improves median and 2-year survival by 2.5 months (from 12.1 to 14.6 months), relative to radiotherapy alone. Although initial treatment can prolong survival, disease progression is almost inevitable, and once a patient progresses through standard first-line therapy, prognosis is very poor. For patients with

recurrent disease, the median survival is 5.0 months [95% confidence interval (CI), 4.6–5.4 months; ref. 3]. Currently, there exists no standard of care for recurrent glioblastoma, although recent survival data from autologous tumor lysate-loaded dendritic cell (DC) vaccination is promising (4). In the era of targeted therapies, clinical studies have demonstrated antitumor activity in patients treated with antiangiogenic agents such as with bevacizumab, a recombinant human mAb against VEGF-A. However, responses with bevacizumab are short, with no notable prolongation in survival (5).

Increasing evidence points to hypoxia as the root cause of angiogenesis and a driving force for resistance to antiangiogenics. In brief, hypoxia-induced factor-1 α subunit (HIF-1 α), normally degradable, is stabilized in hypoxic conditions such that it can dimerize with HIF-1 β and regulate transcription a number of hypoxia-related genes including VEGF (6).

Common alterations involved in the tumorigenesis of glioblastoma, notably EGFR, p53, and PTEN, alter HIF-1 α signaling (7). This gives rise to microvascular hyperplasia, a hallmark of GBM diagnosis. However, unlike normal neovascularizing processes, those involved in GBM are chaotic and do not supply oxygen well (6). Unsurprisingly HIF-1 α expression correlates with both glioma grade and vessel density. Hypoxia in GBM has been shown to promote, rather than impede mitosis, migration, and mutational accumulation (8).

Bevacizumab, through the inhibition of VEGF-A, further exacerbates the hypoxic environment of GBM (9). To better characterize the metabolic changes associated with bevacizumab resistance and other antiangiogenics, we performed metabolomic profiling of tumors and sera from patients with progressive GBM using previously described methods (10, 11). Interestingly, the most significant change that correlated with degree of hypoxia was an increase in the presence of long-chain fatty acids. This finding was not entirely unexpected, as

¹Mays Cancer Center at UT Health San Antonio, San Antonio, Texas. ²Department of Population Health Sciences, Mays Cancer Center, University of Texas Health Science Center at San Antonio, San Antonio, Texas. ³Hematology and Oncology, Florida Cancer Specialists, St. Petersburg, Florida. ⁴The START Center for Cancer Care, Hematology and Oncology, San Antonio, Texas. ⁵Neurosurgery, University of Texas Health Science Center at San Antonio, San Antonio, Texas.

Clinicaltrials.gov Identifier: NCT03032484.

Corresponding Author: Andrew Brenner, Department of Hematology and Oncology, The University of Texas Health Science Center at San Antonio, Mail Code 8232, San Antonio, TX 78229. Phone: 210-450-9000; Fax: 210-692-7502; E-mail: brennera@uthscsa.edu

Clin Cancer Res 2023;29:2419–25

doi: 10.1158/1078-0432.CCR-22-2807

This open access article is distributed under the Creative Commons Attribution-NonCommercial-NoDerivatives 4.0 International (CC BY-NC-ND 4.0) license.

©2023 The Authors; Published by the American Association for Cancer Research

Translational Relevance

There remains a dire need for effective therapeutics for the treatment of recurrent glioblastoma. In this phase II study, modulation of fatty acid synthase (FASN) by the small-molecule inhibitor, TVB-2640 (now known as denifanstat), is investigated. Originally developed for the treatment of nonalcoholic steatohepatitis, the drug is a potent inhibitor of the ketoacylreductase (KR) activity of FASN and has been verified in both murine and phase I study. Current ongoing clinical trials are examining this strategy in non-small cell lung cancer (NSCLC), breast, ovarian, prostate, colon, and pancreatic cancer. Here, TVB-2640 is shown to have favorable safety profile in patients with recurrent glioblastoma and response signals supporting further study in a randomized phase III study.

GBM is known to be a tumor type with large inclusions of fatty acids (i.e., lipid droplets; refs. 12, 13). It has been proposed that these lipid droplets could represent a temporary storage compartment of fatty acids in the form of triglycerides that could in turn serve as reservoir for the tumor cells during times of metabolic stress (14). Recent data using fluorescent labeling of lipid droplets in astrocytes shows restricted mobility in the presence of metabolic stress and inhibition of lipid droplet biogenesis in turn reduces astrocyte abundance (15). It is hypothesized that native astrocytes shuttle and store free fatty acids as a way of decreasing lipotoxicity to neurons (16). During times of limited glucose availability, GBM cells hydrolyze lipid droplets in lysosomes with resultant transfer to mitochondria for β -oxidation (13).

The changes observed in fatty acid content during hypoxia and bevacizumab resistance suggest a potentially targetable mechanism. Fatty acid synthase (FASN) is a homodimeric and multifunctional enzyme that catalyzes the biosynthesis of palmitate in a NADPH-dependent fashion (17). Normal cells in adult tissue ubiquitously express low to moderate levels of FASN; however, these cells, which primarily import lipids from the extracellular milieu, do not have a strict requirement for FASN activity (18). In contrast, tumor cells have an increased requirement for lipids to facilitate membrane biosynthesis, protein modification, and signaling molecules. Consequently, tumor cells are more dependent on *de novo* palmitate synthesis catalyzed by FASN than normal cells (19). In addition, inhibition of FASN increases polyunsaturated fatty acids (PUFA), the accumulation of which may lead to iron-dependent cell death (20). Many solid and hematopoietic tumors overexpress FASN, including non-small cell lung, breast, ovarian, prostate, colon, pancreatic cancers, non-Hodgkin lymphoma as well as GBM (21–29). Moreover, FASN tumor expression has been found to be increased in a stage-dependent manner and correlate with diminished survival (19, 30).

TVB-2640 (denifanstat) is a potent and reversible inhibitor of the FASN enzyme that has been validated in multiple tumor cell lines, as well as in clinical studies (31). TVB-2640 inhibits the ketoacylreductase (KR) enzymatic activity of the FASN enzyme. TVB-2640 has been tested in murine models and a phase I, international, first-in-human, dose-escalation study confirmed predictable pharmacokinetic and tolerable side effects as well as establishing the recommended dose for phase II study (32). There are several ongoing studies of TVB-2640 in KRAS-mutant non-small cell lung cancer (NSCLC), colon cancer, and HER2⁺ advanced breast cancer (33). Preliminary data from patients with breast cancer suggest prolonged disease control when given with cytotoxic chemotherapy (34).

Study rationale

Given the findings of (i) increased hypoxia with bevacizumab, (ii) increased long-chain fatty acid presence in the tumors of patients who have failed bevacizumab, and (iii) evidence suggesting that fatty acid metabolism could play a role in survival under hypoxia, we hypothesized that the addition of TVB-2640 could overcome acquired resistance to bevacizumab. Because progression-free survival (PFS) with bevacizumab is short, we conducted a phase II study in patients with high-grade astrocytoma to evaluate the potential effectiveness and safety of TVB-2640 in combination with bevacizumab.

Patients and Methods

Study design

We conducted a prospective, single-center, open-label phase II study of TVB-2640 plus bevacizumab in patients with high-grade astrocytoma in first relapse who were naïve to bevacizumab. A total of 24 patients were planned to be enrolled. For cycle (C) 1, patients were assigned on a 1:1 ratio to either arm 1 (bevacizumab + TVB-2640) or arm 2 (bevacizumab monotherapy). The purpose of C1 randomization was for exploratory analysis only (see exosome and proteomic analysis). Starting on C2D1, all patients (arms 1 and 2) received bevacizumab /TVB-2640 until development of significant treatment-related toxicity or progressive disease (PD). The local Institutional Review Board (IRB) approved the study, and all patients provided informed written consent before performance of any study-related procedures. The study was conducted in accordance with recognized ethical guidelines (e.g., Declaration of Helsinki, CIOMS, Belmont Report, or U.S. Common Rule).

Eligibility

Adults aged 18 years or older with histologically confirmed high-grade astrocytoma who experienced progression after standard combined modality treatment with radiotherapy plus temozolomide and who had recovered from reversible toxicities of prior therapy were eligible. Of note, this study was designed and initiated prior to World Health Organization Classification of central nervous system (CNS) Tumors, 5th edition, which reclassified GBM, isocitrate dehydrogenase (IDH) mutant (secondary glioblastoma) as astrocyte, IDH-mutant, CNS WHO grade 4. Both IDH wild-type (WT) and IDH-mutant grade 4 astrocytoma were eligible for this study. Patients were required to have an Eastern Cooperative Oncology Group (ECOG) performance status score of 0 to 2 and adequate renal, hepatic, and bone marrow function. Patients were excluded if they were receiving warfarin, enzyme-inducing antiepileptics, or had a history of non-standard radiotherapy, recent investigational agents, biologics, or other cytotoxic agents. Patients with a history of serious intercurrent illness, intracranial hemorrhage, coagulopathy, HIV, or hepatitis were also excluded.

Treatment

In C1, all patients received bevacizumab 10 mg/kg i.v. on D1 and D15. Patients in arm 1 also received TVB-2640 100 mg/m² orally once daily (QD) in C1. After completion of C1, all patients received bevacizumab and TVB-2640 in combination at these same dose regimens. The initial bevacizumab dose was infused over 90 minutes. If the initial infusion was tolerated, the second infusion could be shortened to 60 minutes, and the third and subsequent infusions could have been accordingly shortened to 30 minutes. Dose delays were instituted per standard of care. TVB-2640 was administered by the patient at the same time each day under fasted conditions (i.e., at least 2 hours after last food consumption and at least 1 hour before next food

consumption), with each dose separated by 24 (\pm 4) hours. If a TVB-2640 dose was missed by more than 8 hours, it was not made up.

Safety

Safety assessments included documentation of AEs and serious AEs (SAE), clinical laboratory tests (hematology, clinical chemistry, and urinalysis), physical examinations, ophthalmologic examinations, vital signs, ECOG performance status, and 12-lead electrocardiograms (ECG). Toxicities were graded by the investigator using the NCI Common Terminology Criteria for Adverse Events (NCI CTCAE), version 4.03.

Efficacy

Brain MRI was performed after every even cycle (e.g., C2 or C4) during treatment, with tumor response assessed by the investigator for complete response (CR), partial response (PR) and PD according to the Response assessment in neuro-oncology (RANO) criteria. The same imaging technique was to be used throughout the study. After completion of treatment, patients were followed for survival every 3 months through 1 year after the first dose. Any subsequent antitumor therapy (description and dates) was also documented.

Exosome and proteomic analysis

Before starting and after completion of C1, serum samples were collected for proteomic and lipidomic analyses using standard centrifugation techniques as previously described (35). Relative protein levels in each sample were quantified by normalizing to total peptide-to-spectrum matches (PSM). This was used to represent the percentage of total protein expression for each protein in each sample. After ultracentrifugation, proteomic analysis was conducted at the MD Anderson Proteomic and Metabolomics Facility. In addition, serum was sent for exosome characterization through System Biosciences using defibrination reagent (catalog no. TMEXO-1) and ExoQuick (catalog no. 3EXOQ5A-1) for exosome isolation. Exosome Total RNA isolation was achieved using a SeraMir Exosome RNA Purification Column kit (catalog no. RA808A-1) according to manufacturer's instructions. Final RNA concentration was determined by Agilent Bioanalyzer Small RNA Assay and using Bioanalyzer 2100 Expert instrumentation (Agilent Technologies). Concentration was analyzed in log units base 10. For exosome analysis, exosomes were defined according to 50–120 nm size parameters. For exosome profiling, these samples were processed by System Biosciences using a standard protocol that consisted of Qiagen small RNA library prep, gel purification, and sequencing on Illumina NextSeq SE75. For differential RNA analysis, a mean norm read counts cutoff of 10 was established. A log-fold cutoff was also used to identify targets greater than or equal to +1 and less than or equal to -1 (2-fold change). Accordingly, targets were ranked according to the number of patients whose samples met this cutoff after filtering ($P = 0.01$) for significance, along with FDR controlled for multiple-tests.

Statistical analysis

The primary endpoint was PFS, defined as the time from study enrollment to the first occurrence of relapse, death from any cause, or, in the event of no progression event, until last contact before loss to follow-up. Because of the lack of any systemic therapy with proven survival benefit in the recurrent setting, and the feasibility of this phase II study, a historical control was chosen over contemporaneous arms. Historical data comparisons were made with reference to the phase II BELOB bevacizumab monotherapy (bevacizumab HIS; ref. 36). It was hypothesized that the combination of bevacizumab /TVB-2640 would prolong PFS by 4 months as compared with bevacizumab

historical data. The primary efficacy analyses for estimation of PFS rates was to be performed using a one-sample one-sided log-rank test for an overall type I error at 0.1 and a power of >90% against bevacizumab HIS (BELOB), assuming a median PFS of 7 months with bevacizumab /TVB-2640 and referencing the published bevacizumab HIS median PFS of 3 months and an exponential model. Unless otherwise mentioned, efficacy and safety data for bevacizumab /TVB-2640 refers to the aggregate of arms 1 and 2, because all patients were treated with bevacizumab /TVB-2640 from C2 on. Contrasts of the bevacizumab /TVB-2640 study cohort with historical controls on overall survival (OS) were made with one-sample 1-sided log-rank tests. All other statistical testing was two-sided with a significance level of 5%.

Statistical analyses of safety events were descriptive in nature. Continuous variables were summarized using descriptive statistics (n, mean, SD, median, minimum, and maximum). Categorical variables were summarized showing the number and percentage (n, %) of patients within each classification. Statistical testing, estimates, and CIs were computed with SAS Version 9.4 for Windows (SAS Institute).

Data availability

The data generated in this study are available within the article and its supplementary data files. Raw data for this study were generated at MD Anderson Proteomic and Metabolomics Facility, and System Biosciences. Derived data supporting the findings of this study are available from the corresponding author upon reasonable request. Data types for which community-recognized, structured repository does not exist, or where information could compromise patient privacy or consent, are available upon reasonable request from the corresponding author.

Results

Demographics

Twenty-eight patients were screened with three screen failures for histology, thrombocytopenia, and intracranial bleeding, respectively. A total of 25 patients were enrolled and treated with at least 1 dose of study drug. For the C1 treatment, there were 13 patients randomized to arm 1 (bevacizumab plus TVB-2640) and 12 to arm 2 (bevacizumab monotherapy). Demographics (Table 1; Supplementary Table S1) and participant flow (Supplementary Fig. S1) are summarized. The patient population was well-balanced with regard to sex (52% male). Most (24 patients; 96%) patients were white, with the remaining patient being Asian. Overall, the mean age of patients was 59 years. No significant

Table 1. Patient demographics.

Characteristics	No. (% evaluable)
Mean age (range)	59 (39–87)
Sex/Gender (male)	13 (52)
Baseline ECOG	
0	11 (44)
1	8 (32)
2	6 (24)
Ethnicity/race	
White non-Hispanic	11 (44)
White Hispanic/Spanish/Latino	13 (52)
Asian	1 (4)
Histological features	
IDH WT	19 (90)
MGMT promoter methylation	6 (33)

Abbreviation: WT, wild-type

differences were seen between C1 arms with regard to demographics. All patients had grade 4 astrocytoma. Of the 21 patients with evaluable IDH mutational status, two were IDH mutant (10%). Of the 18 patients with MGMT promoter methylation status, six were methylated (33%).

Safety

TVB-2640 plus bevacizumab was well tolerated with most AEs grade 1 or 2 in intensity (Table 2), including palmar-plantar erythrodysesthesia (PPE), hypertension, mucositis, dry eye, fatigue, and skin infection. Treatment-related grade 3 AEs included four events of PPE and single occurrences of alanine aminotransferase (ALT) elevation, deep venous thrombosis (DVT), hypertension, mucositis, optic neuritis, perirectal abscess, and vomiting. Three of these events (DVT, perirectal abscess, and vomiting) were serious. The only other treatment-related SAE was a single case of aphasia. Two grade 4 AEs, fatigue and hemiplegia, and two grade five AEs, intracranial hemorrhage and sepsis, were reported, all of which were deemed to be unrelated to the study drug.

Efficacy

The PFS6 observed for TVB-2640/bevacizumab was 31.4% and represented a statistically significant improvement in PFS6 over the bevacizumab HIS (16%; $P = 0.008$). Twenty-three patients were evaluable by MRI with two patients being not assessable due to death prior to comparison scans and study withdrawal for patient preference, respectively. The bevacizumab/TVB-2640 median PFS (Fig. 1) was 4.6 months (95% CI, 4.0–6.3) and the median OS (Fig. 2) was 8.9 months (95% CI, 5.2–13.6). A one-sided one-sample log-rank test comparing bevacizumab /TVB-2640 with bevacizumab HIS regarding PFS, computed assuming exponential survival, gave $P = 0.008$ (median 4.5 months, PFS6 = 31.4%), reflecting the larger median PFS in bevacizumab/TVB-2640 relative to bevacizumab HIS (3 months). The corresponding test for OS (bevacizumab HIS median OS = 8 months) gave $P = 0.56$ (median 8.9 months, OS6 = 68%); On the basis of one-sample log-rank testing when compared with bevacizumab HIS (62%). The overall response rate (ORR) for bevacizumab/TVB-2640 was 56% (CR, 17%; PR 39%).

Exosome and proteomic analysis

One patient had no exosome data. Exosome characterization was conducted on serum samples, obtained prior to and following a 28-day cycle of treatment, comparing patients receiving bevacizumab /TVB-2640 with bevacizumab monotherapy (Supplementary Data S1, Supplementary Data S2). Minimal serum protein contamination was detected in samples collected for proteomic analysis. Although serum albumin was present in most samples, it accounted for only a small proportion of the total protein content (<1.3%). In contrast, albumin constituted approximately 50% of plasma proteins, indicating that the proportion of proteins that are serum-derived rather than exosome-derived was relatively small (37). All samples expressed high levels of α -2-macroglobulin (11.4%–69.4%). Galectins are nonglycosylated lectins which regulate formation of vesicles, and their identification is used to confirm exosome presence (38). Galectin-3 binding was also present in all but one sample and accounted for 0.3%–3.7% of all proteins. Taken together, these results suggest exosome purity.

The median size at C1D1 for bevacizumab /TVB-2640 and bevacizumab arms was 112.4 nm (95% CI, 97.6–119) and 107 nm (95% CI, 87.2–115.6), respectively (Supplementary Table S2). The median size at C2D1 for bevacizumab /TVB-2640 and bevacizumab arms was 108.8 nm (95% CI, 88.1–120.1) and 107.55 nm (95% CI, 97.9–123.9), respectively. The median concentration at C1D1 for

bevacizumab /TVB-2640 and bevacizumab arms was 12.66 particles $\times 10^3$ /mL (ref. 8; 95% CI, 12.38–13.1) and 12.65 particles $\times 10^3$ /mL (95% CI, 12–13.1), respectively. The median concentration at C2D1 for bevacizumab /TVB-2640 and bevacizumab arms was 12.64 particles $\times 10^3$ /mL (95% CI, 11.78–13.2) and 12.87 particles $\times 10^3$ /mL (95% CI, 12.28–13.3), respectively. Although no statistically significant difference was observed for either size or concentration (Supplementary Figs. S2 and S3), a decrease in the median concentration of exosomes between C1D1 and C2D1 correlated with increased PFS when both groups were combined on the basis of a proportional hazards model (LogHR = 2.2 ± 0.91 ; HR, 9.1; 95% CI, 1.5–54.4; $P = 0.016$; Supplementary Table S3).

Reactome pathway analysis (reactome.org) was conducted to quantify changes in the relative level of individual proteins between C1 and C2. In patients treated with bevacizumab + TVB-2640 (C1), decreased expression of Annexin A3 (-0.01% of total protein, $P = 0.044$) and A7 (-0.07% of total protein, $P = 0.047$), as compared with bevacizumab monotherapy, was observed.

RNA analysis of exosome contents was also performed. For miRNA analysis of bevacizumab pairwise samples, the upregulated targets of interest (equal or more than 5 samples) were has-miR-338-3, hsa-miR-338, has-miR-4521, hsa-miR-146, hsa-miR-146hasp, hsa-miR-6503, hsa-miR-23b-5p, hsa-miR-4111-5p, hsa-miR-411. For bevacizumab patients, the downregulated targets of interest (equal or more than 5 samples) were hsa-miR-548q, hsa-miR-6877-5p, hsa-miR-6877. For miRNA analysis of TVB/bevacizumab pairwise samples, the upregulated targets of interest (equal or more than 5 samples) were hsa-miR-582. For TVB/bevacizumab patients, there were no downregulated targets of interest (equal or more than 5 samples) which met the predetermined levels of statistical significance.

Discussion

In this phase II study, administration of TVB-2640 plus bevacizumab was found to be well-tolerated with most AEs being of lower grade, and expected. In particular, PPE was commonly observed. Previous research of TVB-2640 in patients with cancer has shown that these symptoms were reversible. Although the pathophysiology of PPE remains poorly understood, eccrine accumulation of chemotherapeutic drugs and epithelial necrosis of eccrine ducts has been implicated but there is no data specific to TVB-2640 on this (39). Interestingly, it has been demonstrated that TVB-2640 results in significant reductions in the saturated and monounsaturated triglyceride content of sebum (34). This fatty acid reduction in sebaceous gland product is likely contributory to PPE.

As there is no systemic therapy with proven survival benefit in the treatment of recurrent GBM, practitioners are faced with the daunting task of extrapolating from what studies have shown the most benefit. Evidence for the utility of bevacizumab comes from two phase II studies which showed PFS6 of 29%–42% (40). The phase II BELOB study was chosen as the comparative arm in this study due to the apparent survival advantage of lomustine plus bevacizumab (PFS6 41%) over bevacizumab monotherapy (16%) observed in that study. However, the subsequent phase III study, EORTC 26101, was unable to confirm the superiority of lomustine plus bevacizumab over lomustine monotherapy (median PFS 4.2 vs. 1.5 months, respectively; ref. 41). With this context in mind, the PFS6 observed for TVB-2640 plus bevacizumab (31.4%) in this study compares favorably with the initial phase II studies of bevacizumab as well the bevacizumab monotherapy arm of BELOB. Although not adequately powered for comparisons of OS, the OS6 observed for TVB-2640 plus bevacizumab compares favorably with those seen in BELOB. Furthermore,

Table 2. Adverse events.

AE	TVB-2640 + bevacizumab (any grade)	TVB-2640 + bevacizumab (grade 3-5)
PPE	18	3
Mucositis	15	1
HTN	13	1
Dry eye	12	0
Fatigue	7	2
Muscle weakness	6	2
Alopecia	5	0
Skin infection	5	0
Arthralgia	4	0
Myalgia	4	0
Elevated ALT	3	1
Allergic rhinitis	3	0
Elevated AST	3	0
Constipation	3	0
Depression	3	0
Dysphasia	3	0
Headache	3	1
Hoarseness	3	0
Paresthesia	3	0
Urinary tract infection	3	1
Back pain	2	0
Cognitive disturbance	2	1
Conjunctivitis	2	0
Diarrhea	2	0
Dry mouth	2	0
Dry skin	2	0
Limb edema	2	0
Hypokalemia	2	1
Pruritus	2	0
Seizure	2	1
Upper respiratory infection	2	0
Acute kidney injury	1	0
Anorexia	1	0
Anxiety	1	0
Aphasia	1	0
Bronchitis	1	0
Catheter-related infection	1	1
Confusion	1	0
Increased creatinine	1	0
Dysesthesia	1	0
Encephalitis	1	1
Conjunctival hemorrhage	1	0
Blepharitis	1	0
Fall	1	0
Flatulence	1	0
Gait disturbance	1	0
Gastritis	1	1
GERD	1	0
Hallucination	1	1
Hyperglycemia	1	1
Hypermagnesemia	1	0
Hypomagnesemia	1	0
Intracranial hemorrhage	1	1
Cerebrovascular ischemia	1	0
Optic neuritis	1	1
Thrombocytopenia	1	0
Proteinuria	1	0
Mood lability	1	0
Rash	1	0
Rectal hemorrhage	1	0

(Continued on the following column)

Table 2. Adverse events. (Cont'd)

AE	TVB-2640 + bevacizumab (any grade)	TVB-2640 + bevacizumab (grade 3-5)
Perirectal pain	1	0
Scalp tenderness	1	0
Sepsis	1	1
Sinusitis	1	0
Candidiasis	1	0
Syncope	1	1
DVT	1	1
Urinary frequency	1	0
Urinary incontinence	1	0
Vomiting	1	1
Watering eyes	1	0
Weight loss	1	0
Perirectal abscess	1	1

Abbreviation: HTN, hypertension.

the high ORR of TVB-2640 plus bevacizumab (56%) including 17% of patients experiencing a CR, suggests that the PFS advantage is not merely due to decreased contrast extravasation from bevacizumab's antiangiogenic effects. Evidence supporting this inference comes from the observation that the ORR for TVB-2640 plus bevacizumab is superior to that seen in the bevacizumab monotherapy arm of BELOB (38%). In aggregate, these results suggest that TVB-2640 plus bevacizumab has activity in GBM which exceeds that of bevacizumab monotherapy. Accordingly, further validation with a larger randomized trial is required. Of note, there is an ongoing trial in China (NCT05118776) investigating TVB-2640 (under the identifier ASC40) in combination with bevacizumab in recurrent glioblastoma.

It is also worth mentioning that, in BELOB, there was suggestion that MGMT status could predict improved PFS and OS for those receiving bevacizumab alone, but not from lomustine or the combination of lomustine plus bevacizumab (table 5 in ref. 36). MGMT promoter methylation is of known prognostic value and predictive

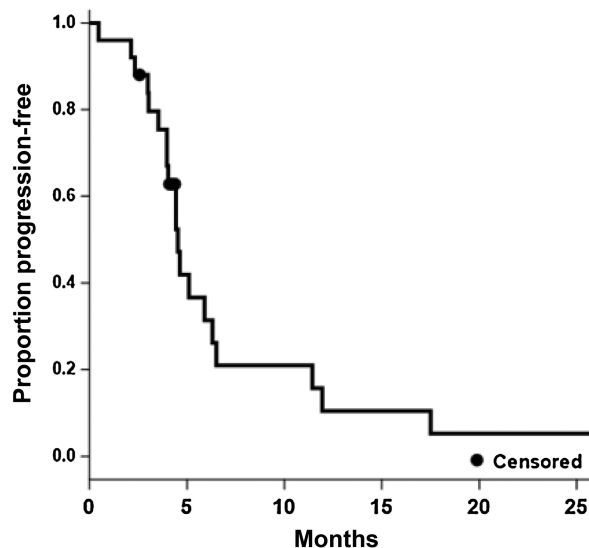


Figure 1. Kaplan-Meier estimate of progression (all patients, N = 25; median = 4.5; 95% CI, 4.0-6.3).

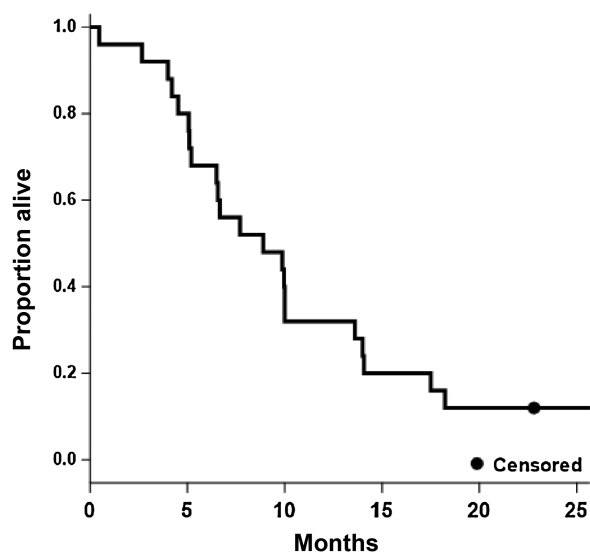


Figure 2.

Kaplan-Meier estimate of OS (all patients, $N = 25$; median = 8.9; 95% CI, 5.2–13.6).

of benefit from temozolomide (42). Although our sample size precluded a dedicated subgroup analysis, we would recommend including methylation, as well as IDH, status as a design variable in any subsequent studies.

A C1 randomization to either TVB-2640 plus bevacizumab or bevacizumab monotherapy was conducted in this trial for biomarker analysis only and was not intended to be comparative for either safety or efficacy. Exosome analysis showed adequate purification as assessed by the proportion of serum to exosome-derived proteins. Neither the size nor concentration of exosomes was found to be statistically different between the arms, suggesting inhibition of FASN does not alter exosome production. However, a statistically superior PFS was observed with decreased exosome concentrations between C1 and C2 when the arms were viewed in aggregate suggesting exosome concentration may be a prognostic biomarker for progression in GBM. This would require larger analysis in conjunction with a phase III study but establishing a correlation between a decrease in exosome concentration before starting therapy and at a later time period could potentially offer prognostic data.

Reactome pathway analysis showed that patients treated with bevacizumab/TVB-2640 for C1 had very marginal decreases in expression of, annexin A3, and A7. Annexin A3 in particular is involved in VEGF signaling (43) and has been previously identified in ovarian cancer exosomes and associated with treatment resistance, but has a mixed role in tumor progression (44, 45). Annexin A7 appears to be a tumor suppressor in glioblastoma, but has also been shown to promote tumor progression in other cancers (46, 47). All considered, these findings suggest a possible interplay between TVB-2640, VEGF signaling and treatment resistance. The RNA analysis of exosomes also highlighted has-miR-582 as being upregulated in patients receiving bevacizumab/TVB-2640. miRNA are single strands of noncoding

RNA that regulate gene expression. The miRNA has-miR-582 has previously been shown to be upregulated in glioblastoma stem cells and promote survival by inhibiting Caspase 3 and 9 (48). Although sRNA prep was used, there was some expression of mRNA fragments (using NCBI RefSeq gene annotation) seen as have previously been described in exosomes. The differential expression analysis of RefSeq results should be interpreted with caution due to the minimal alignment that was observed.

In conclusion, in this phase II study of relapsed high-grade astrocytoma, TVB-2640 was found to be a well-tolerated oral drug that could be safely combined with bevacizumab. The favorable safety profile and efficacy signals support the initiation of larger multicenter trial of TVB-2640 plus bevacizumab in this population.

Authors' Disclosures

W. Kelly reports personal fees from DoD CDRMP Peer Review Panel outside the submitted work. A.E. Diaz Duque reports other support from Lilly, ADCT, AstraZeneca, Genentech, and Morphosys and grants from BMS outside the submitted work. B. Konkel reports grants and nonfinancial support from Sagimet during the conduct of the study. J. Floyd reports grants from NIH and CPRIT during the conduct of the study. A. Brenner reports other support from 3V Biosciences during the conduct of the study as well as grants, personal fees, and nonfinancial support from Plus Therapeutics, grants from Gilead, and personal fees from Seagen outside the submitted work; in addition, A. Brenner has a patent for NanoTx Therapeutics issued, licensed, and with royalties paid from Plus Therapeutics. No disclosures were reported by the other authors.

Authors' Contributions

W. Kelly: Formal analysis, writing—original draft, writing—review and editing. A.E. Diaz Duque: Conceptualization. J. Michalek: Formal analysis. B. Konkel: Investigation. L. Caffisch: Investigation. Y. Chen: Formal analysis. S.C. Pathuri: Formal analysis. V. Madhusudanannair-Kunnuparampil: Investigation. J. Floyd: Investigation. A. Brenner: Conceptualization, formal analysis, supervision, investigation, writing—review and editing.

Acknowledgments

This work was supported by NIH P30 grant (CA054174) as well as an endowment from the S&B Kolitz foundation. The Proteomics and Metabolomics Facility was supported in part by Cancer Prevention Research Institute of Texas (CPRIT) grant no. (RP130397) and NIH grants (1S10OD012304–01, P30CA016672). Biostatistical analysis was supported in part by a CPRIT core facility grant (RP160732). TVB-2640 was provided by Sagimet Biosciences (formerly 3-V Biosciences). The authors thank David Hawke at the MD Anderson Proteomics and Metabolomics Facility. The authors would also like to thank their patients for their trust and participation.

The publication costs of this article were defrayed in part by the payment of publication fees. Therefore, and solely to indicate this fact, this article is hereby marked "advertisement" in accordance with 18 USC section 1734.

Note

Supplementary data for this article are available at Clinical Cancer Research Online (<http://clincancerres.aacrjournals.org/>).

Received December 2, 2022; revised February 13, 2023; accepted April 18, 2023; published first April 24, 2023.

References

1. Stupp R, Hegi ME, Gilbert MR, Chakravarti A. Chemoradiotherapy in malignant glioma: standard of care and future directions. *J Clin Oncol* 2007;25:4127–36.
2. Stupp R, Mason WP, van den Bent MJ, Weller M, Fisher B, Taphoorn MJB, et al. Radiotherapy plus concomitant and adjuvant temozolomide for glioblastoma. *N Engl J Med* 2005;352:987–96.

3. Ballman KV, Buckner JC, Brown PD, Giannini C, Flynn PJ, LaPlant BR, et al. The relationship between six-month progression-free survival and 12-month overall survival end points for phase II trials in patients with glioblastoma multiforme. *Neuro Oncol* 2007;9:29–38.
4. Liao LM, Ashkan K, Brem S, Campian JL, Trusheim JE, Iwamoto FM, et al. Association of autologous tumor lysate-loaded dendritic cell vaccination with extension of survival among patients with newly diagnosed and recurrent glioblastoma: a phase 3 prospective externally controlled cohort trial. *JAMA Oncol* 2023;9:112–21.
5. Friedman HS, Prados MD, Wen PY, Mikkelsen T, Schiff D, Abrey LE, et al. Bevacizumab alone and in combination with irinotecan in recurrent glioblastoma. *J Clin Oncol* 2009;27:4733–40.
6. Domènech M, Hernández A, Plaja A, Martínez-Balibrea E, Balaña C. Hypoxia: the cornerstone of glioblastoma. *Int J Mol Sci* 2021;22:12608.
7. Kaur B, Khwaja FW, Severson EA, Matheny SL, Brat DJ, Van Meir EG. Hypoxia and the hypoxia-inducible-factor pathway in glioma growth and angiogenesis. *Neuro Oncol* 2005;7:134–53.
8. Grimes DR, Jansen M, Macauley RJ, Scott JG, Basanta D. Evidence for hypoxia increasing the tempo of evolution in glioblastoma. *Br J Cancer* 2020;123:1562–9.
9. Xu H, Rahimpour S, Nesvick CL, Zhang X, Ma J, Zhang M, et al. Activation of hypoxia signaling induces phenotypic transformation of glioma cells: implications for bevacizumab antiangiogenic therapy. *Oncotarget* 2015;6:11882–93.
10. Konkel B, Caflisch L, Diaz Duque AE, Brenner AJ. ACTR-25. updated results from a prospective, randomized phase 2 study in patients with first relapse of high-grade astrocytoma using TVB-2640 in combination with avastin versus avastin alone. *Neuro-oncol* 2018;20(suppl_6):vi16.
11. Lodi A, Pandey R, Chiou J, Bhattacharya A, Huang S, Pan X, et al. Circulating metabolites associated with tumor hypoxia and early response to treatment in bevacizumab-refractory glioblastoma after combined bevacizumab and evofosfamide. *Front Oncol* 2022;12:900082.
12. Zoula S, Rijken PFJW, Peters JPW, Farion R, Van der Sanden BPJ, Van der Kogel AJ, et al. Pimonidazole binding in C6 rat brain glioma: relation with lipid droplet detection. *Br J Cancer* 2003;88:1439–44.
13. Wu X, Geng F, Cheng X, Guo Q, Zhong Y, Cloughesy TF, et al. Lipid droplets maintain energy homeostasis and glioblastoma growth via autophagic release of stored fatty acids. *iScience* 2020;23:101569.
14. Remy C, Foulhe N, Barba I, Sam-Lai E, Lahrech H, Cucurella MG, et al. Evidence that mobile lipids detected in rat brain glioma by 1H nuclear magnetic resonance correspond to lipid droplets. *Cancer Res* 1997;57:407–14.
15. Smolič T, Tavčar P, Horvat A, Černe U, Halužan Vasle A, Tratnjek L, et al. Astrocytes in stress accumulate lipid droplets. *Glia* 2021;93:1540–62.
16. Ioannou MS, Jackson J, Sheu S-H, Chang C-L, Weigel AV, Liu H, et al. Neuron-astrocyte metabolic coupling protects against activity-induced fatty acid toxicity. *Cell* 2019;177:1522–35.
17. Maier T, Jenni S, Ban N. Architecture of mammalian fatty acid synthase at 4.5 Å resolution. *Science* 2006;311:1258–62.
18. Shearn CT, Mercer KE, Orlicky DJ, Hennings L, Smathers-McCullough RL, Stiles BL, et al. Short term feeding of a high fat diet exerts an additive effect on hepatocellular damage and steatosis in liver-specific PTEN knockout mice. *PLoS One* 2014;9:e96553.
19. Flavin R, Peluso S, Nguyen PL, Loda M. Fatty acid synthase as a potential therapeutic target in cancer. *Future Oncol* 2010;6:551–62.
20. Bartolacci C, Andreani C, Vale G, Berto S, Melegari M, Crouch AC, et al. Targeting de novo lipogenesis and the Lands cycle induces ferroptosis in KRAS-mutant lung cancer. *Nat Commun* 2022;13:4327.
21. Gouw AM, Eberlin LS, Margulis K, Sullivan DK, Toal GG, Tong L, et al. Oncogene KRAS activates fatty acid synthase, resulting in specific ERK and lipid signatures associated with lung adenocarcinoma. *Proc Natl Acad Sci U S A* 2017;114:4300–5.
22. Al-Bahlani S, Al-Lawati H, Al-Adawi M, Al-Abri N, Al-Dhahli B, Al-Adawi K. Fatty acid synthase regulates the chemosensitivity of breast cancer cells to cisplatin-induced apoptosis. *Apoptosis* 2017;22:865–76.
23. Corominas-Faja B, Vellon L, Cuyas E, Buxó M, Martín-Castillo B, Serra D, et al. Clinical and therapeutic relevance of the metabolic oncogene fatty acid synthase in HER2+ breast cancer. *Histol Histopathol* 2017;32:687–98.
24. Bauerschlag DO, Maass N, Leonhardt P, Verburg FA, Pecks U, Zeppernick F, et al. Fatty acid synthase overexpression: target for therapy and reversal of chemoresistance in ovarian cancer. *J Transl Med* 2015;13:146.
25. Nguyen PL, Ma J, Chavarro JE, Freedman ML, Lis R, Fedele G, et al. Fatty acid synthase polymorphisms, tumor expression, body mass index, prostate cancer risk, and survival. *J Clin Oncol* 2010;28:3958–64.
26. Hamada S, Horiguchi A, Kuroda K, Ito K, Asano T, Miyai K, et al. Increased fatty acid synthase expression in prostate biopsy cores predicts higher Gleason score in radical prostatectomy specimen. *BMC Clin Pathol* 2014;14:3.
27. Zaytseva YY, Harris JW, Mitov MI, Kim JT, Butterfield DA, Lee EY, et al. Increased expression of fatty acid synthase provides a survival advantage to colorectal cancer cells via upregulation of cellular respiration. *Oncotarget* 2015;6:18891–904.
28. Bian Y, Yu Y, Wang S, Li L. Up-regulation of fatty acid synthase induced by EGFR/ERK activation promotes tumor growth in pancreatic cancer. *Biochem Biophys Res Commun* 2015;463:612–7.
29. Gelebart P, Zak Z, Anand M, Belch A, Lai R. Blockade of fatty acid synthase triggers significant apoptosis in mantle cell lymphoma. *PLoS One* 2012;7:e33738.
30. Menendez JA, Lupu R. Fatty acid synthase and the lipogenic phenotype in cancer pathogenesis. *Nat Rev Cancer* 2007;7:763–77.
31. Jones SF, Infante JR. Molecular pathways: fatty acid synthase. *Clin Cancer Res* 2015;21:5434–8.
32. Falchook G, Infante J, Arkenau H-T, Patel MR, Dean E, Borazanci E, et al. First-in-human study of the safety, pharmacokinetics, and pharmacodynamics of first-in-class fatty acid synthase inhibitor TVB-2640 alone and with a taxane in advanced tumors. *Eclinicalmedicine* 2021;34:100797.
33. ClinicalTrials.gov. (2020). TVB-2640. Available at <https://clinicaltrials.gov/CT2/results?cond=&term=TVB-2640&cntry=&state=&city=&dist=>. Accessed October 19, 2020.
34. Brenner AJFG, Patel M, Infante JR, Arkenau HT, Dean EM, et al. Abstract P6-11-09: Heavily pre-treated breast cancer patients show promising responses in the first in human study of the first-in-class fatty acid synthase (FASN) inhibitor, TVB-2640 in combination with paclitaxel. *Cancer Res* 2017;77:6-11-09.
35. Onódi Z, Pelyhe C, Terézia Nagy C, Brenner GB, Almási L, Kittel Á, et al. Isolation of high-purity extracellular vesicles by the combination of iodixanol density gradient ultracentrifugation and bind-elute chromatography from blood plasma. *Frontiers in Physiology* 2018;9:1479.
36. Taal W, Oosterkamp HM, Walenkamp AME, Dubbink HJ, Beerepoot LV, Hanse MCJ, et al. Single-agent bevacizumab or lomustine versus a combination of bevacizumab plus lomustine in patients with recurrent glioblastoma (BELOB trial): a randomised controlled phase 2 trial. *Lancet Oncol* 2014;15:943–53.
37. Farrugia A. Albumin usage in clinical medicine: tradition or therapeutic? *Transfus Med Rev* 2010;24:53–63.
38. Bänfer S, Jacob R. Galectins in intra- and extracellular vesicles. *Biomolecules* 2020;10:1232.
39. Chidharla A, Kanderi T, Kasi A. Chemotherapy acral erythema (palmar-plantar erythrodysesthesia, palmoplantar erythrodysesthesia, hand-foot syndrome). *StatPearls* 2020.
40. Kreisl TN, Kim L, Moore K, Duic P, Royce C, Stroud I, et al. Phase II trial of single-agent bevacizumab followed by bevacizumab plus irinotecan at tumor progression in recurrent glioblastoma. *J Clin Oncol* 2009;27:740–5.
41. Wick W, Gorlia T, Bendszus M, Taphoorn M, Sahm F, Harting I, et al. Lomustine and bevacizumab in progressive glioblastoma. *N Engl J Med* 2017;377:1954–63.
42. Hegi ME, Diserens A-C, Gorlia T, Hamou M-F, de Tribolet N, Weller M, et al. MGMT gene silencing and benefit from temozolomide in glioblastoma. *N Engl J Med* 2005;352:997–1003.
43. Park JE, Lee DH, Lee JA, Park SG, Kim N-S, Park BC, et al. Annexin A3 is a potential angiogenic mediator. *Biochem Biophys Res Commun* 2005;337:1283–7.
44. Yin J, Yan X, Yao X, Zhang Y, Shan Y, Mao N, et al. Secretion of annexin A3 from ovarian cancer cells and its association with platinum resistance in ovarian cancer patients. *J Cell Mol Med* 2012;16:337–48.
45. Wu N, Liu S, Guo C, Hou Z, Sun MZ. The role of annexin A3 playing in cancers. *Clin Transl Oncol* 2013;15:106–10.
46. Pan S-J, Zhan S-K, Ji W-Z, Pan Y-X, Liu W, Li D-Y, et al. Ubiquitin-protein ligase E3C promotes glioma progression by mediating the ubiquitination and degradation of Annexin A7. *Sci Rep* 2015;5:11066.
47. Grewal T, Wason SJ, Enrich C, Rentero C. Annexins - insights from knockout mice. *Biol Chem* 2016;397:1031–53.
48. Floyd DH, Zhang Y, Dey BK, Kefas B, Breit H, Marks K, et al. Novel anti-apoptotic microRNAs 582-5p and 363 promote human glioblastoma stem cell survival via direct inhibition of caspase 3, caspase 9, and Bim. *PLoS One* 2014;9:e96239.